

Petrography, geochemistry, and tectonics of a rifted fragment of Mainland Asia: evidence from the Lasala Formation, Mindoro Island, Philippines

R. A. B. Concepcion · C. B. Dimalanta ·
G. P. Yumul Jr · D. V. Faustino-Eslava ·
K. L. Queaño · R. A. Tamayo Jr · A. Imai

Received: 1 September 2010 / Accepted: 22 January 2011 / Published online: 27 February 2011
© Springer-Verlag 2011

Abstract Petrological and geochemical investigations of the sedimentary Lasala formation in northwest Mindoro, Philippines, offer new insights into the origin of this geologically contentious region. Mindoro island's position at the boundary between Sundaland and the Philippine Mobile Belt has led to variable suggestions as to how much of it is continent derived or not. The Eocene Lasala formation overlies the Jurassic Halcon metamorphics, a regionally metamorphosed suite generally thought to have formed as a result of arc-continent collision processes. The sedimentary formation consists mainly of sandstones and

shales interbedded with mudstones, basalt flows, and subordinate limestones and conglomerates. Petrographic information on the Lasala clastic rocks demonstrates a uniform framework composition that is predominantly quartzose. Major oxide, trace element abundances, and various elemental ratios similarly impart a strongly felsic signature. These characteristics are taken to indicate a chiefly continental, passive margin derivation and deposition of the Lasala sediments during the Eocene. The weak indication of active margin influence is suggested to be an inherited signature, supported by paleogeographic models of the southeastern Asian margin area during the pre-Cenozoic.

R. A. B. Concepcion · C. B. Dimalanta ·
G. P. Yumul Jr · D. V. Faustino-Eslava (✉) · R. A. Tamayo Jr
Rushurgent Working Group—Tectonics and Geodynamics
Group, College of Science, National Institute of Geological
Sciences, University of the Philippines, Diliman,
Quezon City, Philippines
e-mail: dei_faustino@yahoo.com

G. P. Yumul Jr
Department of Science and Technology,
Bicutan, Taguig City, Philippines

K. L. Queaño
Mines and Geosciences Bureau—Central Office,
Department of Environment and Natural Resources,
North Avenue, Diliman, Quezon City, Philippines

K. L. Queaño
Earth and Materials Science and Engineering Department,
Mapua Institute of Technology, Intramuros, Manila, Philippines

A. Imai
Department of Earth Resources Engineering,
Kyushu University, Fukuoka, Japan

A. Imai
Department of Earth Science and Technology,
Akita University, Akita, Japan

Keywords Major and trace elements · Passive margin · Palawan microcontinent · Mindoro · Philippines

Introduction

In recent years, much of the progress made in provenance research of sedimentary rocks has been in the geochemical examination of these rocks as a complementary tool to petrographic analysis. Although sedimentary rocks cannot abscond from factors such as chemical weathering, sediment recycling, metamorphism and other diagenetic process (McLennan 1982; Nesbitt and Young 1996; Nesbitt et al. 1996), trace elements such as Ce, Cs, Co, La, Nb, Sc, Ta, Ti, V, Y, and Zr that are known for their low mobility and low residence time in water (Fedó et al. 1996; Liu et al. 2007; Rahman and Suzuki 2007), usually preserve the original source rock characteristics and therefore can be useful provenance and tectonic setting indicators. Furthermore, rare earth elements (REE) are relatively stable and are least affected by chemical

weathering and can therefore supplement the trace elements in retaining the source rock properties of a sedimentary suite (Reatigui et al. 2005; Kasanzu et al. 2008). As a result, recent geochemical studies of sedimentary rocks have been applied in plate tectonic delineation and reconstructions (Moss 1998; Asiedu et al. 2000; Suzuki et al. 2000; Tam et al. 2005; van Hattum et al. 2006). For instance, Gu et al. (2002) successfully presented that the suturing of the Yangtze and Cathaysia blocks in South China did not occur until the Late Proterozoic time as evidenced by the geochemical characteristics of the Hunan Proterozoic turbidites. In northwest Panay, Philippines, geochemical signatures of the Buruanga Peninsula clastic rocks suggest a silicic provenance in contrast with the Antique Range mafic provenance that is just adjacent to it. Such information helped delineate the extent of the continental fragment in this part of the Philippines (e.g., Gabo et al. 2009).

In the Philippines, numerous studies have been carried out in western central Philippines to delineate the juxtaposition of two primary tectonostratigraphic terranes: the Philippine Mobile Belt which is a seismically active region of island arc affinity and the aseismic Palawan continental block that migrated from the southern margin of Mainland Asia during the mid-Oligocene as a consequence of the Eocene to Miocene opening of the South China Sea (Fig. 1a) (Taylor and Hayes 1983; Hall 2002; Hsu et al. 2004). Mindoro island, being situated in the western part of central Philippines, has long been investigated for its part

in the collision zone. Two contrasting models exist on how much of the island is, in fact, continental in character (Fig. 1b). One model proposes that only the southwestern portion is associated with the Palawan continental block and that the remaining region belongs to the Philippine Mobile Belt (Hamilton 1979; Taylor and Hayes 1983; Sarewitz and Karig 1986). Hashimoto and Sato (1968) suggested that Mindoro has a pre-Jurassic basement since it is unconformably overlain by the ammonite-bearing continent-derived mid- to upper Jurassic Mansalay Formation. Furthermore, Sarewitz and Karig (1986) believed that a high-angle NW–SE structural boundary termed as the Mindoro Suture Zone that divides the island into two: the Mindoro block and the North Palawan block (Fig. 1b). They further argued that exposures of the Mansalay Formation were only restricted within the lower block (southeastern portion) of the island. The second model, however, suggests that the whole Mindoro island is of continental affinity (Holloway 1982; Rangin et al. 1985; Bird et al. 1993; Yumul et al. 2008). However, this recognition was based largely on structural and geophysical data.

To determine the more viable model, an examination of the Late Eocene Lasala Formation, the oldest sedimentary sequence in northwestern Mindoro (Hashimoto and Sato 1968; MMAJ-JICA 1984; Faure et al. 1989), is carried out. In particular, the petrographic and geochemical attributes of this formation are presented in this study, providing new insights into the geological evolution of this part of the

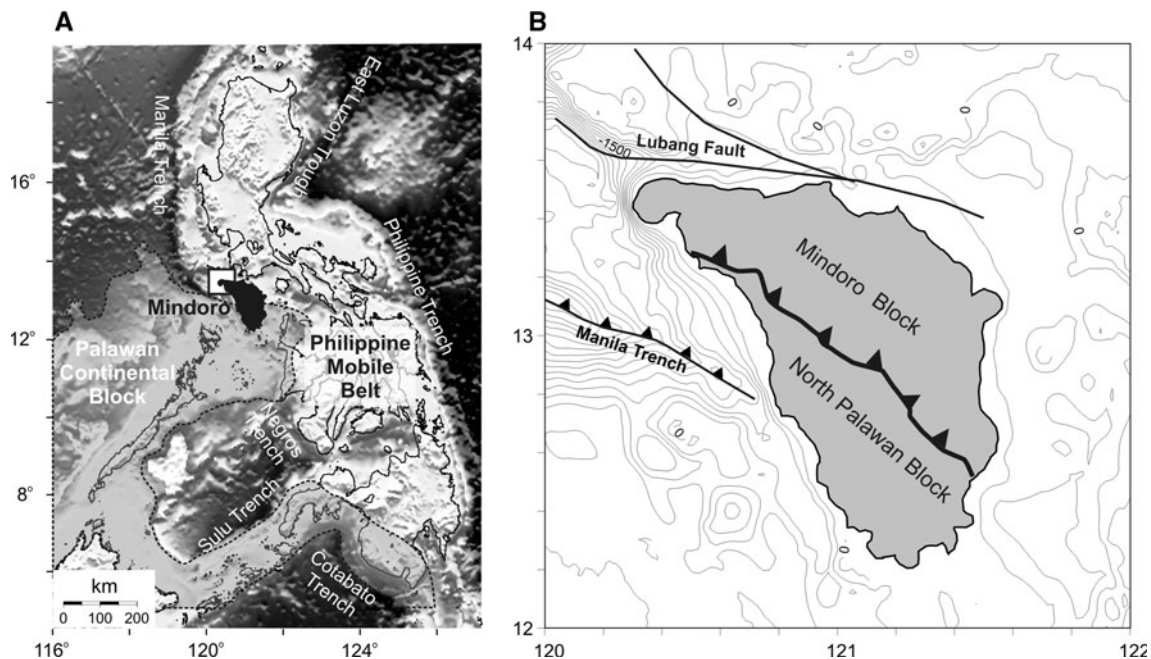


Fig. 1 Mindoro Island in central Philippines has long been an area of interest especially in the light of its possible role during the collision between the Palawan continental block (gray area bounded by broken

lines) and the Philippine Mobile Belt (unshaded area). The northwestern tip of Mindoro Island (boxed area) was the site of this geological/geochemical/geophysical investigation

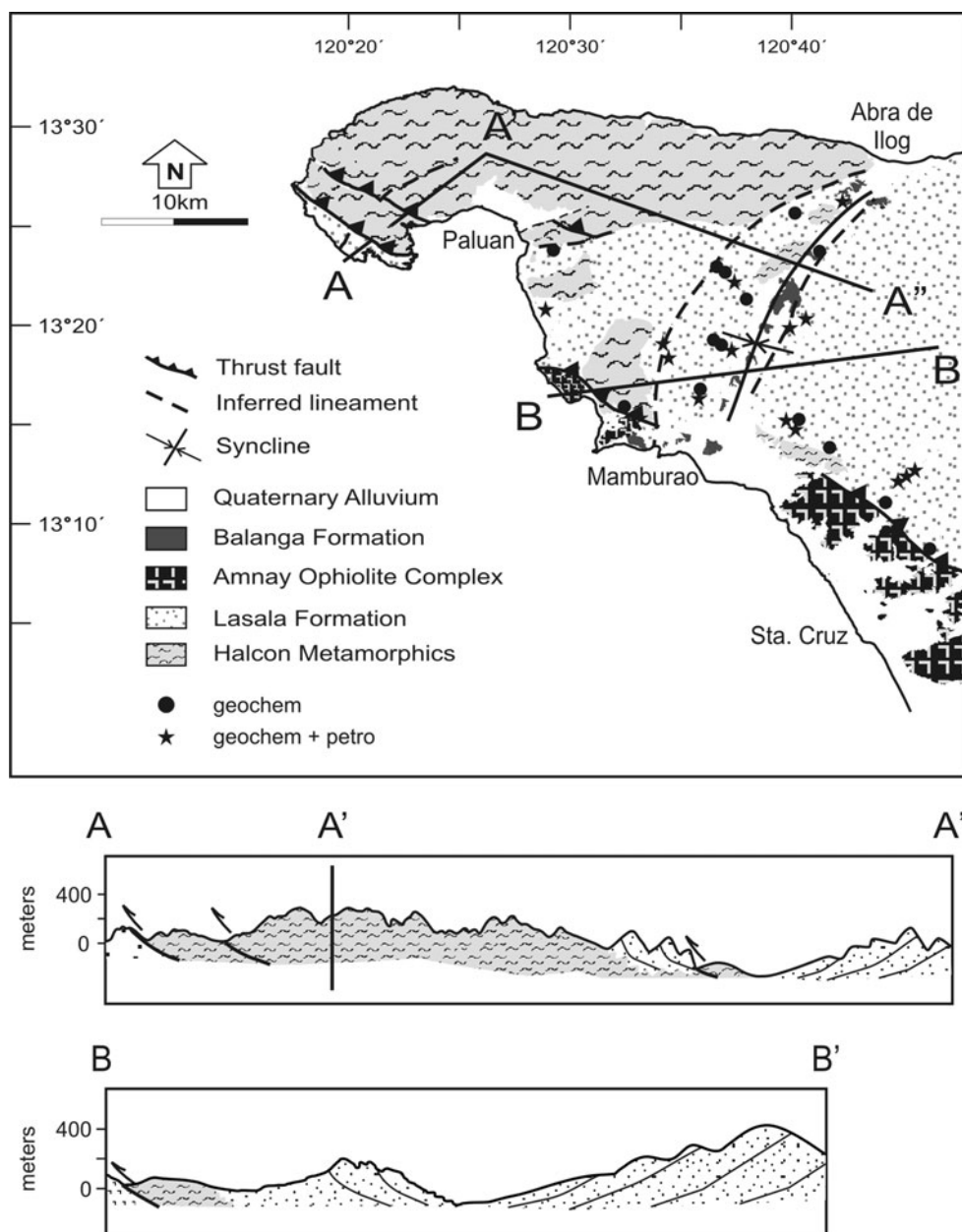
Philippine island arc system and assisting in the delineation of the extent of the boundary of the arc-continent collision in the country.

Geology of northwest Mindoro

The island of Mindoro lies to the south of Luzon along the western edge of the Philippine Mobile Belt abutting Sundaland. Its position at this collision boundary is instrumental to the preservation of various terranes on the island. In northwest Mindoro, the oldest of these terranes is the Jurassic Halcon metamorphics that is widely exposed in Paluan, Abra de Ilog, and Mamburao (Teves 1954;

Hashimoto and Sato 1968). It consists mostly of chlorite, quartz mica, talc–chlorite, and graphite schists with minor phyllitic metasediments (Fig. 2). Exposures of extremely sheared and pervasively serpentinized harzburgites, isotropic gabbros, sheeted dikes, and pillow basalts were previously mapped as the Mangyan Series. However, recent mapping revealed that these crust–mantle units to occur as mega blocks within the Halcon metamorphics. Thus, we interpret these megablocks to have been incorporated into the Halcon metamorphics before it underwent regional metamorphism. As such, it appears that the Halcon metamorphics was originally a mélange, consisting of sedimentary, volcanic, and ophiolitic materials, which was subjected to regional metamorphism sometime after the

Fig. 2 Recent mapping revealed that northwest Mindoro comprises of a metamorphic complex (Halcon metamorphics), ophiolite complex (Amnay Ophiolite Complex), an Eocene (Lasala Formation) and Plio-Pleistocene tuffaceous (Balanga Formation) sedimentary sequences. Sample location of the clastic rocks from the Lasala Formation in northwest Mindoro which were subjected to petrographic and geochemical analyses is also shown



Cretaceous period. Unconformable on the Halcon metamorphics is the sedimentary Eocene Lasala Formation (Fig. 2). This sedimentary unit is extensively exposed as interbeds of medium-grained sandstones and mudstones with minor basalt flows, conglomerates, and limestones. This is the oldest sedimentary sequence in northwest Mindoro and was deposited prior to the collision of the Palawan continental block with the Philippine Mobile Belt. In thrust, contact with both the Halcon metamorphics and the Lasala Formation is the Middle Oligocene Amnay Ophiolite Complex that is strewn along the western coast of northwest Mindoro in a northwest–southeast trend (Fig. 2). This emplaced oceanic lithosphere exposes residual peridotites and pyroxenites, isotropic and cumulate gabbros, dike complex, pillow lavas, and pelagic mudstones. Because of its age and location, the Amnay Ophiolite Complex is believed to represent an onramped piece of the South China Sea crust (Rangin et al. 1985; Jumawan et al. 1998; Yumul et al. 2009). Capping all these older units is the Plio-Pleistocene Balanga Formation (Agadier-Zepeda et al. 1992) that is limited in exposure to low-lying areas, particularly along the northeast–southwest basin connecting Abra de Ilog and Mamburao (Fig. 2). This sedimentary unit consists of interbedded tuffaceous sandstones and siltstones with minor conglomerates and coralline limestones.

Lasala formation

The Lasala Formation was first reported by Hashimoto (1981) for the sequence of rocks exposed along Lasala River in northern Mindoro. The sequence is made up of gray sandstone that is rhythmically interbedded with dark gray shale. Minor conglomerates, mudstones, and limestones are also observed along with basalt flows. Foraminifera (*Pellatispira mirabilis*, *Operculina* cf. *saipanensis*, *Amphistegina radiata*, *Rotalidae* sp. and *Spherogypsina* sp.) from the limestone found in Lubang island limits the age of this formation to Late Eocene (Faure et al. 1989). In the study area, it specifically outcrops along the rivers of Abra de Ilog, Liwliw, Sinambalan and Mamburao rivers in the east, along Talusungan, Tuay, Mamara, Maalis-is, and Tuguilan rivers in the west and along Sta, and Cruz and Pagbahan rivers in the south (Fig. 2). An exposure of this formation in northern part of Mindoro is considered as the type section for the Lasala Formation. Very good exposures of this unit were also mapped along the Pagbahan River in northwest Mindoro.

Outcrops of the Lasala Formation along the Pagbahan River are approximately 50 m in height and extend up to 200 m. Beds vary in thickness from less than a centimeter to about 50-cm-thick beds. Sandstone beds encountered along the Pagbahan River strike NE and dip NW. Outcrops were also observed along Tuguilan River. These consist of

fine- to medium-grained sandstone and shale interbeds. The sandstone beds are approximately 0.5-meters thick and the shale beds vary in thickness from 3 to 5 cm. The beds strike N60–85°W and dip 30–50°NE.

The fine-grained clastic rocks (0513-PAG-02, 040408-7A-LF, 0407-DVF-7, 0512-MAAL-05, 0407-KLQ-7, 0404-KLQ-7A) that include dark gray shales and red mudstones yielded fossils that assigned a Late Eocene—earliest Oligocene age to the Lasala Formation. The presence of the calcareous nannofossils taxa *Sphenolithus* spp., *Coccolithus pelagicus*, *Cyclicargolithus floridanus*, *Dictyococcites bisectus/Reticulofenestra bisecta*, and *Reticulofenestra umbilicam* was noted (Table 1). These nanno-organisms suggest a deep marine environment that received influence from sediment inflow coming from the shallow portions of the sea.

Sampling and analytical methods

Medium-grained sandstone samples from the Lasala Formation were examined petrographically. At least 400 grains were counted per sample to identify the proportions of quartz, feldspar, and lithic fragments present. Adopting the Gazzi–Dickinson method, the grains are separated into fine (diameter < 0.0625 mm) and coarse components (diameter > 0.0625 mm) (Table 2). The point count data are plotted on total quartz-feldspar-lithic (Qt-F-L) and monocrystalline quartz-feldspar-total lithic (Qm-F-Lt) diagrams. These diagrams are used to discriminate among sandstones deposited in different provenance terranes (Dickinson and Suczek 1979). Samples collected during the fieldwork comprise mudstones, fine- to medium-grained sandstones. Thirty-six of the collected samples were trimmed to remove weathered surfaces and were subsequently crushed in a jaw crusher to reduce their size to approximately 1.0 mm. The crushed fragments were pulverized in an agate crusher and were coned and quartered. Approximately 2.0 g of each powdered sample were sent to the Department of Earth Resource Engineering, Kyushu University, Japan, to determine the major element compositions using a Rigaku RIX 3100 X-Ray Fluorescence spectrometer. The analysis was carried out following the procedure of Soejima (1999). Seventeen of these samples were analyzed for trace and rare earth element compositions using an inductively coupled plasma—mass spectrometer at the Chemex Laboratory. The major and trace element compositions of representative samples are shown in Table 3. Accuracy is 1% for major elements, and detection limits for trace and rare earth elements range from 0.01 to 10,000 ppm. Loss on ignition (LOI) was determined from the weight loss after the samples were dried in the oven at 1,050°C for 2 h. Several samples analyzed at the National Taiwan University and University of Hongkong are also included in the plots.

Table 1 Nanofossil assemblages of the Lasala Formation

| | Faure et al. (1989) | MMAJ-JICA (1984) | 2009 This study ^a | 0407-KLQ-7 | 0404-KLQ-7A | 0513-PAG-02 | 040408-7A | 0407-DVF-7 | 0512-MAAL-5 |
|------------|--|---------------------------------------|--|---------------------------------------|---|---|---|---|---|
| Assemblage | <i>Pellastispira mirabilis</i> | <i>Halkyardia minima</i> | <i>Globigerina</i> spp. | <i>Globigerina</i> spp. | <i>Globigerina</i> spp. | <i>Sphenolithus</i> spp. | <i>Cyclicargolithus floridanus</i> | <i>Sphenolithus</i> spp. | <i>Cyclicargolithus floridanus</i> |
| | <i>Operculina</i> cf. <i>saipanensis</i> | <i>Biplanispira mirabilis</i> | <i>Catapsydrax dissimilis</i> | <i>Globigerina praebulloides</i> | <i>Dietyococites bisectus/ Reticulofenestra bisecta</i> | <i>Coccolithus pelagicus</i> | <i>Cyclicargolithus floridanus</i> | <i>Cyclicargolithus floridanus</i> | <i>Dietyococites bisectus/ Reticulofenestra bisecta</i> |
| | <i>Amphistegina radiata</i> | <i>Globorotalia (T.) increbescens</i> | <i>Globorotalia ampliapertura</i> | <i>Globigerina tripartite</i> | <i>Cyclicargolithus floridanus</i> | <i>Sphenolithus</i> spp. | <i>Coccolithus pelagicus</i> | <i>Coccolithus pelagicus</i> | <i>Sphenolithus</i> spp. |
| | <i>Rotalidae</i> sp. | <i>Globigerina</i> | <i>Catapsydrax dissimilis</i> | <i>Catapsydrax dissimilis</i> | <i>Helicosphaera compacta</i> | <i>Dietyococites bisectus/ Reticulofenestra bisecta</i> | <i>Dietyococites bisectus/ Reticulofenestra bisecta</i> | <i>Dietyococites bisectus/ Reticulofenestra bisecta</i> | |
| | <i>Spherogypsina</i> sp. | | <i>Globigerina angiporoides</i> | <i>Globigerina cf. Tapuricensis</i> | <i>Cyclicargolithus</i> cf. <i>C. abisectus</i> | <i>Reticulofenestra umbilica</i> | <i>Reticulofenestra umbilica</i> | <i>Clausiococcus fenestratus</i> | |
| | | | <i>Globigerina</i> cf. <i>Tapuricensis</i> | <i>Globorotalia (T.) increbescens</i> | | <i>Ericsonia formosa</i> | <i>Ericsonia formosa</i> | <i>Ericsonia formosa</i> | |
| | | | | | | <i>Clausiococcus fenestratus</i> | <i>Reticulofenestra umbilica</i> | <i>Reticulofenestra umbilica</i> | |
| Age | Late eocene | Eocene | Late eocene to early oligocene | Late eocene to early oligocene | | | | | |
| Env. | | | Deep marine | Deep marine | | | | | <i>Zygrhablithus bijugatus</i> |

MMAJ-JICA (1984) proposed an Eocene age for this sedimentary suite while a Late Eocene age was suggested by Faure et al. (1989). Samples obtained from recent mapping (2009) contained nanofossil taxa that yielded a Late Eocene to Early Oligocene age

^a Analyzed by A.G.S. Fernando (Nannoworks Laboratory, National Institute of Geological Sciences) and E.Y. Mula and R.T.C. Ancog (Mines and Geosciences Bureau)

Table 2 Point-count data of Lasala clastic rocks

| Sample | Locality | Mean grain size (mm) | Classification | Modal | | | Normalized | | | | | | Normalized | | | Matrix Cement (%) | | | |
|---------------|--------------|----------------------|-------------------------|-------|-----|-----|------------|----|----|----|-----------------------|--------|------------|-------|--------|-------------------|-------|--------|----|
| | | | | Qm | Qp | Qt | F | Lv | Ls | Lm | Other detrital grains | Qt (%) | F (%) | L (%) | Qm (%) | | F (%) | Lt (%) | |
| 0412-GRP5-4 | Pagbahan | 0.15 | Arkose | 78 | 7 | 85 | 106 | 3 | 3 | 0 | 2 | 43 | 54 | 3 | 40 | 54 | 7 | 3 | 11 |
| 0409-RAT-4 | Mamara | 0.2 | Lithic wacke | 64 | 75 | 139 | 7 | 3 | 6 | 0 | 4 | 90 | 5 | 6 | 41 | 5 | 54 | 34 | 2 |
| 0407-KLQ4-B | Paluan | 0.5 | Quartz arenite | 181 | 91 | 272 | 10 | 5 | 0 | 0 | 3 | 95 | 3 | 2 | 63 | 3 | 33 | 11 | 0 |
| 0414-GRP2-1 | Tuguilan | 0.3 | Lithic wacke | 81 | 137 | 218 | 7 | 12 | 5 | 0 | 3 | 90 | 3 | 7 | 33 | 3 | 64 | 20 | 0 |
| 0414-GRP7-4 | Tuay | 0.4 | Subarkose | 175 | 24 | 199 | 40 | 1 | 0 | 0 | 0 | 83 | 17 | 0 | 73 | 17 | 10 | 11 | 18 |
| 0409-KLQ-1 | Cabacao | 0.15 | Lithic wacke | 113 | 34 | 147 | 23 | 77 | 0 | 0 | 17 | 60 | 9 | 31 | 46 | 9 | 45 | 19 | 0 |
| 0412-GRP4-6 | Pagbahan | 0.2 | Feldspathic wacke | 24 | 127 | 151 | 25 | 0 | 0 | 0 | 0 | 86 | 14 | 0 | 14 | 14 | 72 | 43 | 0 |
| 0411-GRP2-3 | Tayamaan | 0.15 | Quartz arenite | 214 | 19 | 233 | 14 | 8 | 0 | 0 | 24 | 91 | 5 | 3 | 84 | 5 | 11 | 8 | 3 |
| 0411-GRP3-6 | Liwliw | 0.7 | Feldspathic litharenite | 33 | 61 | 94 | 37 | 13 | 48 | 0 | 0 | 49 | 19 | 32 | 17 | 19 | 64 | 18 | 15 |
| 0408-JAG-2 | Cabiguhan | 0.5 | Lithic arenite | 19 | 166 | 185 | 1 | 77 | 33 | 0 | 32 | 63 | 0 | 37 | 6 | 0 | 93 | 1 | 0 |
| 0412-LTA-8 | Pagbahan | 0.2 | Arkose | 164 | 17 | 181 | 93 | 0 | 5 | 0 | 7 | 65 | 33 | 2 | 59 | 33 | 8 | 2 | 5 |
| 0408-11 | Cabacao | 0.2 | Lithic wacke | 147 | 41 | 188 | 1 | 11 | 12 | 0 | 0 | 89 | 0 | 11 | 69 | 0 | 30 | 31 | 0 |
| 0512-ADI-18 | Abra de Ilog | 0.2 | Arkosc wacke | 126 | 20 | 146 | 69 | 2 | 2 | 0 | 8 | 67 | 32 | 2 | 58 | 32 | 11 | 22 | 0 |
| 0412-GRP4-7 | Pagbahan | 0.2 | Subarkose | 160 | 124 | 284 | 10 | 0 | 26 | 0 | 33 | 89 | 3 | 8 | 50 | 3 | 47 | 2 | 3 |
| 0407-LTA-2 | Tuguilan | 0.3 | Subarkose | 142 | 105 | 247 | 18 | 1 | 12 | 0 | 6 | 89 | 6 | 5 | 51 | 6 | 42 | 4 | 6 |
| 0408-KLQ-1 | Talusungan | 0.2 | Quartz arenite | 201 | 51 | 252 | 12 | 12 | 0 | 0 | 16 | 91 | 4 | 4 | 73 | 4 | 23 | 15 | 2 |
| DRCC-041008-4 | Mamburao | 0.3 | Lithic arkose | 88 | 42 | 130 | 65 | 22 | 5 | 0 | 34 | 59 | 29 | 12 | 40 | 29 | 31 | 13 | 6 |
| 0415-GRP2-2 | Mamburao | 0.4 | Quartz arenite | 230 | 23 | 253 | 12 | 3 | 0 | 0 | 23 | 94 | 4 | 1 | 86 | 4 | 10 | 11 | 0 |
| 0413-GRP3-1 | Mamburao | 0.5 | Subarkose | 61 | 112 | 173 | 34 | 2 | 0 | 0 | 22 | 83 | 16 | 1 | 29 | 16 | 55 | 19 | 8 |

Quantitative analysis of the detrital components shows high amounts of quartz grains for most of the samples

Qmu monocrySTALLINE quartz, *Qp* polycrySTALLINE quartz, *F* feldspar, *Lv* lithic volcanics, *Ls* lithic sedimentary, *Lm* lithic metamorphics

Table 3 Geochemical compositions of representative samples from the Eocene Lasala Formation

| | ARC-041108-12* | 0407-RAT-3 | 0409-KLQ-1 | 0412-GRP5-4 | 0512-TALU-19 | 0512-WOMM-11 | MIN-0411-GRP2-3 | MIN-0408-KQ-1 | 0409-RAT-4 | 0412-GRP4-6 | 0414-GRP7-4 | 0414-GRP2-1 | 0512-ADI-17 | 0411-GRP3-6 | 0407-KQ-4 | 0408-JAG-2 | 040408-07** |
|--------------------------------|----------------|------------|------------|-------------|--------------|--------------|-----------------|---------------|------------|-------------|-------------|-------------|-------------|-------------|-----------|------------|-------------|
| <i>Oxides (wt%)</i> | | | | | | | | | | | | | | | | | |
| SiO ₂ | 77.09 | 71.38 | 69.27 | 73.37 | 74.04 | 48.13 | 73.47 | 73.65 | 69.40 | 62.51 | 68.93 | 72.85 | 69.37 | 78.44 | 81.77 | 64.88 | 47.54 |
| TiO ₂ | 0.63 | 0.56 | 0.63 | 0.44 | 0.57 | 0.33 | 0.46 | 0.57 | 0.40 | 0.66 | 0.27 | 0.47 | 0.58 | 0.38 | 0.38 | 0.92 | 0.16 |
| Al ₂ O ₃ | 10.45 | 13.30 | 15.01 | 9.84 | 12.86 | 8.87 | 11.27 | 9.78 | 17.50 | 13.07 | 10.35 | 11.18 | 16.85 | 9.07 | 9.54 | 12.49 | 18.76 |
| FeO | 3.86 | 2.91 | 3.66 | 3.56 | 3.04 | 1.81 | 3.95 | 3.41 | 1.47 | 4.35 | 2.66 | 5.09 | 1.68 | 3.11 | 1.68 | 6.24 | 4.55 |
| MnO | 0.07 | 0.05 | 0.03 | 0.25 | 0.07 | 0.09 | 0.06 | 0.10 | 0.01 | 0.14 | 0.13 | 0.08 | 0.01 | 0.09 | 0.01 | 0.14 | 0.10 |
| MgO | 1.14 | 4.49 | 2.83 | 2.93 | 2.02 | 1.32 | 2.08 | 2.51 | 0.97 | 3.26 | 1.59 | 3.13 | 1.06 | 1.96 | 0.91 | 4.65 | 10.11 |
| CaO | 0.25 | 0.40 | 0.19 | 4.55 | 0.38 | 31.96 | 0.67 | 2.57 | 0.12 | 4.36 | 5.72 | 0.42 | 0.07 | 0.39 | 0.10 | 2.30 | 16.53 |
| Na ₂ O | 2.20 | 2.66 | 0.05 | 2.10 | 1.61 | 1.84 | 2.57 | 1.68 | 1.24 | 1.38 | 3.03 | 1.64 | 2.98 | 2.08 | 2.11 | 2.27 | 1.06 |
| K ₂ O | 1.78 | 0.62 | 3.68 | 0.67 | 2.44 | 1.78 | 2.29 | 1.47 | 4.89 | 2.54 | 1.15 | 1.36 | 4.10 | 1.19 | 1.39 | 1.43 | 0.00 |
| P ₂ O ₅ | 0.13 | 0.15 | 0.17 | 0.08 | 0.11 | 0.07 | 0.08 | 0.11 | 0.03 | 0.18 | 0.08 | 0.17 | 0.05 | 0.11 | 0.06 | 0.18 | 0.03 |
| LOI | 1.85 | 3.41 | 4.35 | 2.13 | 2.75 | 3.63 | 2.99 | 4.05 | 3.80 | 7.41 | 5.97 | 3.24 | 3.11 | 3.11 | 2.02 | 4.40 | 1.36 |
| Total | 99.44 | 99.93 | 99.87 | 99.92 | 99.89 | 99.83 | 99.89 | 99.90 | 99.83 | 99.86 | 99.88 | 99.63 | 99.86 | 99.93 | 99.97 | 99.90 | 100.19 |
| <i>Trace elements (ppm)</i> | | | | | | | | | | | | | | | | | |
| Ba | 302.60 | 77.50 | 339.00 | 101.00 | 307.00 | 344.00 | 452.00 | 127.00 | 594.00 | 308.00 | 154.00 | 147.50 | 751.00 | 109.50 | 113.50 | 133.00 | |
| Ce | 54.83 | 110.00 | 86.40 | 41.40 | 58.30 | 39.50 | 27.90 | 53.40 | 39.00 | 58.30 | 35.80 | 32.70 | 80.40 | 23.20 | 31.20 | 27.50 | |
| Co | 9.50 | 5.90 | 6.60 | 12.60 | 6.00 | 7.70 | 6.60 | 6.70 | 0.60 | 9.20 | 4.40 | 11.20 | 0.90 | 2.90 | 2.00 | 14.80 | |
| Cr | 65.43 | 50.00 | 50.00 | 40.00 | 50.00 | 30.00 | 20.00 | 50.00 | 20.00 | 60.00 | 40.00 | 80.00 | 20.00 | 30.00 | 20.00 | 120.00 | |
| Cs | | 0.54 | 3.07 | 2.82 | 3.05 | 1.77 | 0.93 | 2.00 | 3.68 | 6.01 | 1.58 | 2.72 | 1.57 | 1.30 | 2.07 | 1.64 | |
| Cu | 13.62 | 5.00 | 11.00 | 5.00 | 10.00 | 13.00 | 15.00 | 9.00 | 7.00 | 14.00 | 7.00 | 25.00 | <5 | 14.00 | <5 | 24.00 | |
| Dy | 3.42 | 3.01 | 10.50 | 4.07 | 3.00 | 2.23 | 2.05 | 3.13 | 1.09 | 3.61 | 2.35 | 3.52 | 3.80 | 1.59 | 2.24 | 3.77 | |
| Er | 1.80 | 1.67 | 4.33 | 2.10 | 1.83 | 1.42 | 1.27 | 1.86 | 0.80 | 2.10 | 1.24 | 1.89 | 2.12 | 1.05 | 1.39 | 2.30 | |
| Eu | 0.97 | 1.27 | 3.86 | 1.21 | 0.73 | 0.63 | 0.56 | 0.79 | 0.36 | 1.13 | 0.70 | 0.94 | 1.19 | 0.40 | 0.62 | 0.99 | |
| Ga | 12.21 | 13.00 | 13.00 | 10.80 | 11.90 | 9.40 | 9.90 | 8.50 | 12.20 | 14.00 | 8.50 | 11.40 | 15.80 | 8.20 | 7.30 | 12.90 | |
| Gd | 4.20 | 6.22 | 15.15 | 4.85 | 4.28 | 2.51 | 2.29 | 4.16 | 1.61 | 4.76 | 3.05 | 4.20 | 5.30 | 1.75 | 2.81 | 3.98 | |
| Hf | 5.09 | 4.50 | 4.70 | 3.90 | 5.40 | 3.60 | 3.30 | 7.50 | 3.90 | 4.50 | 3.00 | 2.10 | 8.00 | 2.70 | 3.10 | 2.60 | |
| Ho | 0.66 | 0.54 | 1.74 | 0.79 | 0.59 | 0.46 | 0.43 | 0.64 | 0.24 | 0.72 | 0.47 | 0.70 | 0.74 | 0.34 | 0.46 | 0.79 | |
| La | 27.64 | 57.90 | 91.90 | 20.10 | 31.20 | 15.10 | 14.90 | 26.90 | 21.20 | 30.00 | 18.80 | 16.70 | 45.60 | 11.60 | 17.00 | 15.60 | |
| Lu | 0.28 | 0.26 | 0.43 | 0.26 | 0.27 | 0.21 | 0.20 | 0.28 | 0.15 | 0.28 | 0.18 | 0.26 | 0.32 | 0.18 | 0.20 | 0.30 | |
| Nb | 11.64 | 7.60 | 8.00 | 7.40 | 6.60 | 4.00 | 3.30 | 6.50 | 4.50 | 10.00 | 4.00 | 5.40 | 6.20 | 3.40 | 3.60 | 6.50 | |
| Nd | 24.69 | 47.30 | 77.20 | 20.20 | 25.10 | 13.50 | 12.60 | 22.80 | 13.80 | 25.30 | 14.70 | 17.20 | 33.10 | 9.60 | 13.90 | 15.70 | |
| Ni | 26.31 | 24.00 | 76.00 | 32.00 | 18.00 | 18.00 | 17.00 | 22.00 | <5 | 31.00 | 17.00 | 37.00 | 8.00 | 15.00 | 8.00 | 59.00 | |
| Pb | 14.68 | <5 | 13.00 | 9.00 | 14.00 | 15.00 | 6.00 | 12.00 | 10.00 | 13.00 | 13.00 | 8.00 | 8.00 | 11.00 | <5 | 6.00 | |
| Pr | 6.84 | 13.25 | 20.40 | 5.05 | 6.95 | 3.64 | 3.46 | 6.14 | 4.17 | 6.85 | 4.06 | 4.22 | 9.46 | 2.63 | 3.79 | 3.82 | |
| Rb | 69.59 | 11.80 | 93.50 | 34.10 | 67.80 | 59.80 | 47.90 | 40.40 | 116.50 | 80.50 | 34.70 | 45.50 | 105.50 | 36.80 | 40.70 | 36.50 | |

Table 3 continued

| | ARC-041108-12* | 0407-RAT-3 | 0409-KLQ-1 | 0412-GRP5-4 | 0512-TALU-19 | 0512-WOMM-11 | MIN-0411-GRP2-3 | MIN-0408-KQ-1 | 0409-RAT-4 | 0412-GRP4-6 | 0414-GRP7-4 | 0414-GRP2-1 | 0512-ADI-17 | 0411-GRP3-6 | 0407-KQ-4 | 0408-JAG-2 | 040408-07** |
|----|----------------|------------|------------|-------------|--------------|--------------|-----------------|---------------|------------|-------------|-------------|-------------|-------------|-------------|-----------|------------|-------------|
| Sm | 4.64 | 8.16 | 16.60 | 4.77 | 4.46 | 2.60 | 2.48 | 4.44 | 2.06 | 4.86 | 3.05 | 4.09 | 5.70 | 1.99 | 2.81 | 3.74 | |
| Sn | | 3.00 | 2.00 | 2.00 | 2.00 | 1.00 | 1.00 | 2.00 | 1.00 | 2.00 | 1.00 | 1.00 | 2.00 | 1.00 | 1.00 | 3.00 | |
| Sr | 53.04 | 90.30 | 28.50 | 147.50 | 78.70 | 101.00 | 101.50 | 58.60 | 44.70 | 124.50 | 258.00 | 54.70 | 98.20 | 68.60 | 44.40 | 81.30 | |
| Ta | 0.92 | 0.80 | 0.80 | 0.60 | 0.70 | 0.40 | 0.40 | 0.70 | 0.50 | 0.80 | 0.40 | 0.50 | 0.70 | 0.30 | 0.40 | 0.60 | |
| Tb | 0.59 | 0.72 | 2.23 | 0.77 | 0.56 | 0.40 | 0.36 | 0.58 | 0.20 | 0.68 | 0.44 | 0.67 | 0.74 | 0.28 | 0.42 | 0.65 | |
| Th | 7.85 | 7.94 | 8.53 | 6.22 | 8.39 | 5.71 | 5.53 | 8.02 | 7.37 | 8.12 | 6.50 | 4.84 | 14.65 | 4.45 | 5.25 | 3.54 | |
| Tm | 0.26 | 0.24 | 0.51 | 0.28 | 0.26 | 0.21 | 0.19 | 0.26 | 0.12 | 0.27 | 0.16 | 0.26 | 0.30 | 0.16 | 0.18 | 0.29 | |
| U | 1.98 | 1.41 | 1.84 | 1.54 | 1.73 | 1.24 | 1.11 | 1.72 | 1.37 | 1.77 | 1.91 | 1.33 | 2.87 | 1.07 | 1.30 | 0.98 | |
| V | 45.95 | 45.00 | 48.00 | 48.00 | 44.00 | 41.00 | 39.00 | 31.00 | 32.00 | 55.00 | 24.00 | 91.00 | 35.00 | 42.00 | 38.00 | 112.00 | |
| W | | 1.00 | 2.00 | 1.00 | 2.00 | 1.00 | 1.00 | 1.00 | 1.00 | 2.00 | 1.00 | 1.00 | 1.00 | 1.00 | 1.00 | 1.00 | |
| Y | 17.18 | 13.50 | 42.10 | 21.80 | 16.00 | 12.10 | 11.40 | 17.20 | 6.40 | 19.70 | 12.70 | 19.20 | 20.10 | 8.50 | 12.60 | 22.60 | |
| Yb | 1.75 | 1.68 | 3.10 | 1.77 | 1.80 | 1.48 | 1.29 | 1.80 | 0.93 | 1.92 | 1.18 | 1.68 | 2.03 | 1.14 | 1.24 | 1.96 | |
| Zn | 53.90 | 31.00 | 90.00 | 81.00 | 46.00 | 42.00 | 19.00 | 34.00 | 14.00 | 61.00 | 34.00 | 68.00 | 23.00 | 31.00 | 27.00 | 70.00 | |
| Zr | 201.10 | 166.00 | 179.00 | 144.00 | 217.00 | 142.00 | 130.00 | 301.00 | 147.00 | 162.00 | 115.00 | 76.00 | 297.00 | 110.00 | 119.00 | 99.00 | |

Major elements are in wt%. Trace and rare earth elements are in ppm. *041108-12 was analyzed at the University of Hongkong, and **040408-07 was performed at the National Taiwan University

Results

Petrography

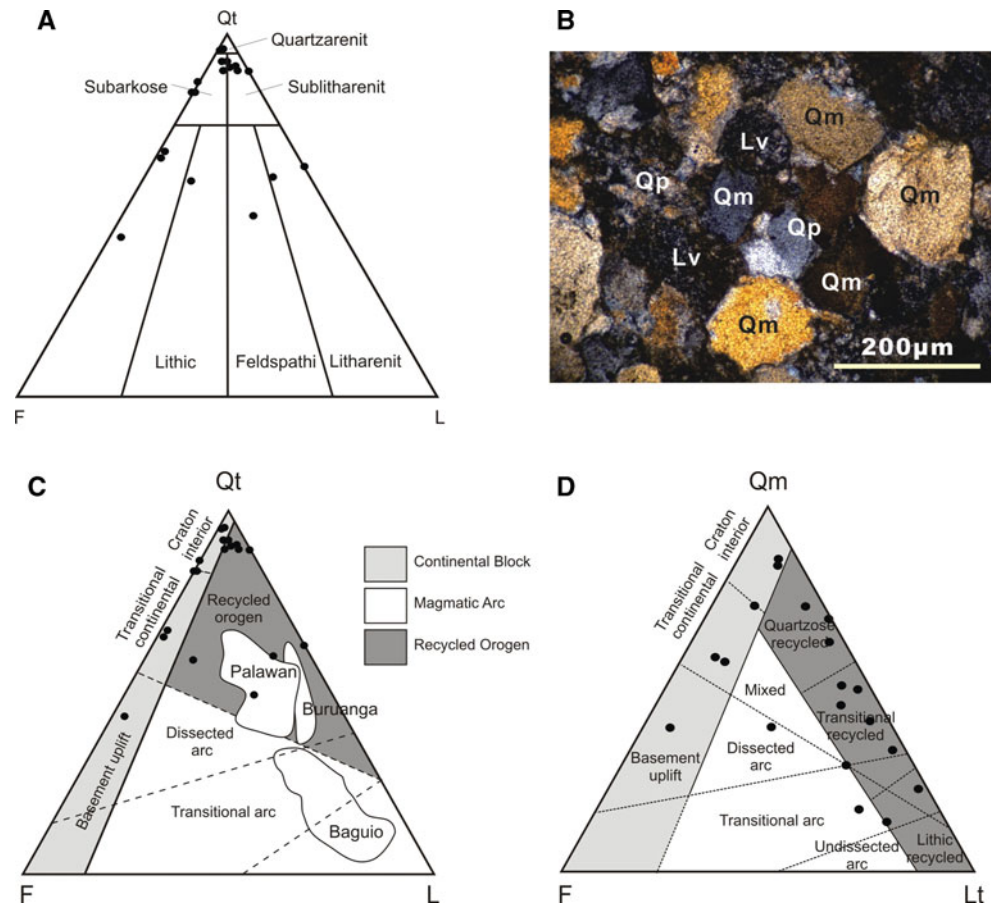
Compositional variations between sandstone suites can be determined through the use of ternary diagrams, the most common of which are the Qt-F-L and Qm-F-Lt diagrams of Dickinson (1985). Plots of the Lasala clastic rocks in these diagrams provide useful information regarding their source rocks and provenance terranes that can aid in understanding the geologic history of Mindoro Island, in general, and northwest Mindoro, in particular. Samples that were subjected to petrographic analysis consist of medium-grained sandstones that were mostly collected along Tuguilan, Mamara, Liwliw, Maalis-is, Talusungan, and Pagbahan rivers (Fig. 2). Twenty samples were carefully chosen ensuring that they are of almost similar grain sizes in order to maintain coherence and to avoid misleading results, as framework minerals in very fine-grained sandstones are so minute that sometimes they are regarded as part of the matrix. Three (0412-LTA-8, 0412-GRP4-6, 0412-GRP4-7) out of the 20 samples were gathered along the Pagbahan River. Results of the petrographic examination were plotted in the sandstone nomenclature diagram of Folk (1965). Due to the high content of quartz minerals compared with other components, most of the samples are classified as sublitharenites, arkoses, and quartz arenites (Fig. 3a, b).

The samples are generally medium-grained with grain sizes ranging from 0.15 to 0.7 mm. Angular to subangular grains are embedded in 16% average clay matrix. Furthermore, the samples generally contain 5% cement and this is commonly in the form of carbonates and quartz overgrowth. In terms of composition, majority of the samples consist of quartz (50–95%). Most of these are monocrystalline (45–80%) but several samples (e.g., 0412-GRP4-6, 0408-JAG-2, 0411-GRP2-3 and 0415-GRP2-2), containing abundant polycrystalline (55–70%) quartz minerals and few monocrystalline quartz grains (10–30%). Feldspars in the samples, which exhibit prominent twinning and sometimes zoning, have a wide range of abundance (0.5–30%). Albite and oligoclase are the most common feldspars present. Some of these plagioclases have already been partially altered to calcite.

A small amount (2–12%) of lithic component is observed and is predominantly in the form of basaltic fragments. Some sedimentary rock fragments are also observed composed mainly of chert. Other detrital rock components present in the samples include opaque minerals and micas.

Modal analyses of the Lasala sandstones were plotted using the ternary discrimination diagrams of Dickinson (1985) (Fig. 3c). The point count data indicate two major provenance terranes. In the Qt-F-L diagram, most of the

Fig. 3 **a** Using the sandstone classification diagram of Folk (1965), the Lasala samples (solid circles) are mostly classified as sublitharenites, arkoses, and quartz arenites. **b** Photomicrograph of a representative sample (0412-GRP4-7) showing abundant quartz minerals. Qm-quartz monocrystalline; Qp-quartz polycrystalline; Lv-lithic volcanic fragment. **c** On the Qt-F-L (b) and Qm-F-Lt (d) diagrams of Dickinson (1985), the Lasala Formation clastic rocks plot mostly within the continental block (craton interior, transitional continental) and recycled orogen fields



samples fall under the craton interior and transitional continental, whereas nine samples occupy the recycled orogen field. In the Qm-F-Lt diagram where quartz polycrystalline (Qp) minerals are counted as lithic fragments, the same provenance terranes emerged (Fig. 3d).

Geochemistry

Relatively high SiO_2 contents (62.5–87%) characterize the clastic rocks of the Lasala Formation (Table 3). The TiO_2 values are distributed within a narrow range (0.16–0.90%), but a wide spread is observed in the values of Al_2O_3 (5–17.5%) and MgO (0.70–4.65%). One sample (0409-RAT-11) displays unusually high MgO contents (~10%). Most of the samples have low MnO (<1%) and Na_2O (0.05–3%) values. The FeO plus MgO contents vary from ~1.5 to 7% with $\text{Na}_2\text{O}/\text{K}_2\text{O}$ ranging from 0.01 to 6. The Mindoro Lasala sandstone samples are characterized by similarly high SiO_2 contents as the Cretaceous to Eocene Palawan sandstones (73–81%) and the Buruanga, northwest Panay clastic rocks (65–85%). The Palawan samples have TiO_2 concentration between 0.15 and 0.30%, Al_2O_3 is from ~9 to 11% but low MnO (<0.1%) and MgO (<0.7%) contents. In the case of the Buruanga clastic rocks, TiO_2 ranges from 0.30 to 1.00%, Al_2O_3 is 7–17%, MnO

0.02–0.10, and MgO 0.30–2.7% (e.g., Suzuki et al. 2000; Gabo et al. 2009).

Various ratios are used as indicators of the original composition of the source rocks. One such ratio is the $\text{Al}_2\text{O}_3/\text{TiO}_2$ that ranges from 3 to 8 for mafic rocks, 8–21 for intermediate rocks, and from 21 to 70 for felsic rocks (e.g., Nagarajan et al. 2007). This is based on the assumption that sedimentary rocks derived from an island-arc setting usually contain more Ti-bearing mafic phases such as biotite, chlorite, and ilmenite and less Al-bearing minerals (e.g., plagioclase) than continent-derived sediments (Chakrabarti et al. 2009). With $\text{Al}_2\text{O}_3/\text{TiO}_2$ varying from 14 to 44, derivation from intermediate to felsic source rocks is inferred for the Lasala clastic rocks. The Buruanga samples are similarly characterized by $\text{Al}_2\text{O}_3/\text{TiO}_2$ from 15 to 47, whereas the Palawan samples have a little bit higher $\text{Al}_2\text{O}_3/\text{TiO}_2$ ratios from 35 to 64 (e.g., Suzuki et al. 2000; Gabo et al. 2009).

Among the trace elements, Co, Ni, Cr, Sc, and V and the ratios Cr/Ni and Ni/Co have been utilized as indicators of ferromagnesian minerals. These elements are compatible during igneous fractionation processes. Hence, these trace elements are generally enriched in mafic to ultramafic rocks but are generally depleted in felsic rocks (e.g., Hunstman-Mapila et al. 2005; Kawano et al. 2006). The

Lasala sandstone samples have variable but generally low abundances of Co (0.6–15 ppm), Cr (20–120 ppm), Ni (8–76 ppm), and V (24–112 ppm). These concentrations are comparable with upper crustal and post-Archean average shale values that contain <30 ppm Co, <120 ppm Cr, <100 ppm Ni, and <150 ppm V (e.g., Taylor and McLennan 1985). The low abundances of these ferromagnesian trace elements, therefore, indicate the minimal contribution of mafic components in the source rocks (e.g., Gu et al. 2002; Armstrong-Altrin and Verma 2005). Overall, the geochemical characteristics of the Lasala clastic rocks suggest derivation chiefly from a continental source.

Discussion

Weathering history of the source area

Chemical weathering which sedimentary rocks undergo strongly influences their mineralogy and geochemical characteristics (e.g., Nesbitt and Young 1982; Faundez et al. 2002; Mongelli et al. 2006). The most common indicator of weathering as a result of the chemical changes that took place in the source area is the Chemical Index of Alteration (CIA) proposed by Nesbitt and Young (1982), which is defined as $\text{Al}_2\text{O}_3/(\text{Al}_2\text{O}_3 + \text{CaO}^* + \text{Na}_2\text{O} + \text{K}_2\text{O}) \times 100$ (molar contents, with CaO^* being CaO content in silicate fraction of the sample). This index accounts for the amounts of mobile cations such as K^+ , Ca^+ , Na^+ as well as the less mobile cations such as Al^{3+} that are present in the samples. High CIA values imply increasing removal of K, Ca, and Na relative to the more stable Al cation, and these consequently reflect the intensity of weathering. Fresh rocks that experience nearly absent to very little chemical alteration have CIA values ranging from 50 to 60, whereas those that are close to 100 indicate intense weathering (e.g., Fedo et al. 1995; Lee and Lee 2003; Kasanzu et al. 2008; Liang et al. 2009).

The Lasala clastic rock samples generally indicate a moderately weathered source area with CIA values ranging from 60 to 77. Grain size poses a major effect on the calculated CIA values of the samples. Mudstones tend to have been subjected to extreme weathering conditions compared with sandstones so higher CIA values are usually associated with mudstones and finer-grained sandstones, whereas coarser sandstones show lower values (e.g., McLennan et al. 1980; Faundez et al. 2002). This grain size correlation is demonstrated by the Lasala samples as finer clastic rocks show high values (69–77) whereas coarser sandstones register lower values (60–68) (Fig. 4).

In the $\text{Al}_2\text{O}_3 - (\text{Na}_2\text{O} + \text{CaO}) - \text{K}_2\text{O}$ (A-CN-K) ternary diagram (Fig. 4), a best fit line drawn through the data

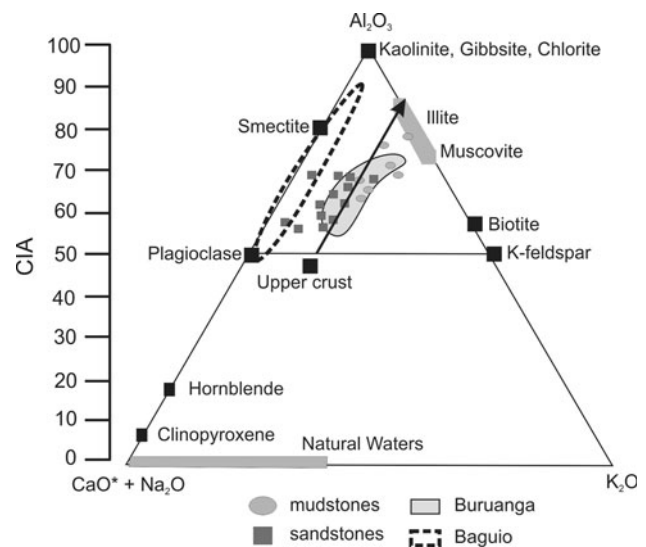


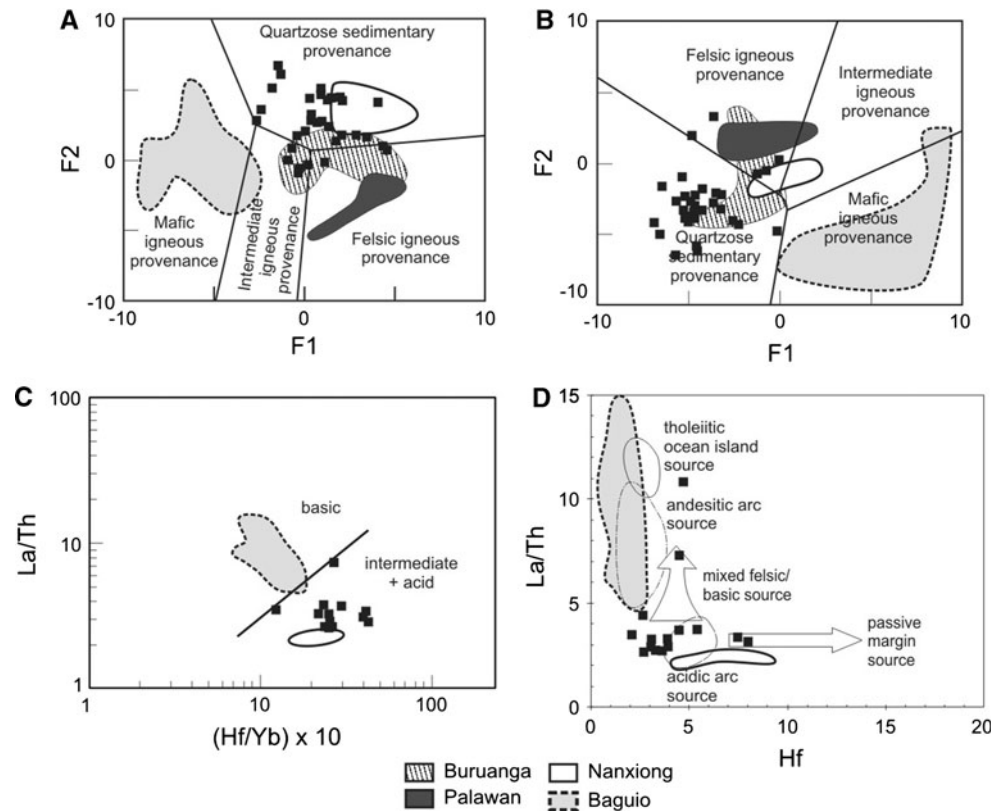
Fig. 4 The chemical index of alteration (CIA) values for the Lasala mudstones and sandstones vary from 60 to 77. The *solid arrow* corresponds to the ideal weathering trend extending from an upper continental crust composition toward the A–K join to illite. UCC composition is from Taylor and McLennan (1985)

runs almost parallel to the ideal weathering trend. Lasala clastic rocks that lie above the ideal weathering trend reflect the scarcity of alkali feldspars in these samples (Fedo et al. 1995; Deru et al. 2007). Petrographic examination shows that plagioclase crystals make up most of the feldspar grains. Several samples, especially the mudstones, plot toward the K-apex and exhibit CIA ratios slightly lower than the premetasomatized trend that indicates mild post-depositional K-metasomatism (Fedo et al. 1995; Faundez et al. 2002; Lee 2009; Hossain et al. 2010). However, this post-depositional effect is only restricted to the Lasala mudstones.

Nature of source rocks

The A-CN-K diagram helps discern the nature of the source area composition. The best fit line through the Lasala samples connects to the plagioclase—alkali feldspar join where a higher proportion of plagioclase compared with alkali feldspar is noted (Fig. 4). This is indicative of a granodiorite source composition consistent with what is reported for the upper continental crust (e.g., Fedo et al. 1995; Deru et al. 2007). Moreover, two discriminant diagrams that are helpful in the classification of the provenance of a sedimentary suite have been proposed by Bhatia (1983) and Roser and Korsch (1988). Calculated discriminant function scores (F1, F2) of the samples are plotted within the four established source rock fields based on TiO_2 , Al_2O_3 , MgO , CaO , Na_2O , and K_2O . The majority of the Lasala clastic rocks when plotted on these diagrams occupy the quartzose sedimentary and felsic igneous

Fig. 5 a, b Function diagrams proposed by (a) Bhatia (1983) and (b) Roser and Korsch (1988) to discriminate the nature of source rocks. A quartzose sedimentary and felsic igneous provenance for the Mindoro clastic rocks (black square) is suggested by the plots. Buruanga (stripes), Palawan (black), Nanxiong (white), and Baguio (gray) fields were plotted for comparison. **c** On the La/Th versus $(\text{Hf}/\text{Yb}) \times 10$ diagram, the Lasala samples plot in the intermediate to acidic provenance field. The fields for Baguio (gray) and Nanxiong Basin (white) samples are shown for comparison. **d** The same result is noted when the samples are plotted using the La/Th versus Hf diagram with the Mindoro samples clustering near the acidic arc source field. The fields for Baguio (gray) and Nanxiong Basin (white) samples are shown for comparison



discriminant fields in both diagrams (Fig. 5a, b). This result represents derivation from granite-gneiss basement terranes and quartz-rich sedimentary rocks that make up a continental crust (Tucker 2001; van Hattum et al. 2006). These kinds of rocks are characterized by abundant felsic minerals such as quartz and feldspars. Petrographic analysis confirms these findings as the samples that are noted to be dominantly quartzose. A high proportion of quartzose material usually implies a continental source area (e.g., Crook 1974; Roser and Korsch 1986, 1988; Tucker 2001; Rahman and Suzuki 2007; Yan et al. 2007). It is also important to note that a few of the samples fall within the intermediate igneous provenance field in the second diagram. This is because these samples contain more Ti-bearing minerals (e.g., biotite, chlorite) than the other samples, and so their calculated function discrimination scores are different from the rest of the samples. This could indicate that, in addition to the dominantly felsic or quartzose source rocks of the Mindoro Lasala clastic rocks, island arc rocks were also being eroded and their detritus were incorporated in the Lasala Formation.

The fields for the clastic rocks from Palawan and Buruanga Peninsula, which recent studies propose to be part of the Palawan microcontinental block, are shown in these discrimination diagrams (Fig. 5a, b). The Palawan clastic rocks occupy the felsic igneous provenance field whereas the Buruanga clastic rocks generally plot within

the felsic igneous provenance and quartzose recycled provenance fields and occupy the same fields as the Lasala samples. To further ascertain the continental provenance of the Lasala clastic rock samples as suggested by the discrimination function diagrams, plots of the Nanxiong Basin sedimentary rocks (from Yan et al. 2007) from South China, which is where the Palawan continental block is believed to have been derived, are also incorporated as fields in these diagrams. The Nanxiong Basin samples plot within the quartzose sedimentary, felsic igneous, and intermediate igneous provenance fields of the Roser and Korsch discriminant diagram (Fig. 5a, b). Samples from the Klondyke Formation in Baguio, Northern Luzon, are also plotted in these diagrams. The Baguio clastic rocks, which are derived from an oceanic island arc source, fall clearly within the mafic igneous provenance fields in stark contrast to the continent-derived sedimentary units (e.g., Tam et al. 2005; Yumul et al. 2008).

In addition to major element compositions, trace element data are also useful indicators of provenance. The continental character of the samples is substantiated by the La/Th versus $(\text{Hf}/\text{Yb}) \times 10$ and La/Th versus Hf plots (Fig. 5c, d). It is an inherent property of the continental crust to have high Th. This reflects its Proterozoic transition from a relatively undifferentiated mafic upper crustal

composition to a more differentiated felsic composition. It is expected that the La/Th ratio will be low (<5) in continental rocks but elevated in mafic rocks (Meinhold et al. 2007; Chakrabarti et al. 2009). The clastic rocks from the Lasala Formation are generally characterized by La/Th ranging from 2.6 to 7.3. Other examples of clastic rocks sourced from quartzose sedimentary rocks in a continental margin setting are the Buruanga clastic rocks from northwest Panay and the Tertiary sedimentary units from the Nanxiong Basin in South China. The Buruanga samples are characterized by La/Th from 1.5 to 5, whereas the latter samples have ratios of ~ 2 . In contrast, clastic rocks from an oceanic island arc source like the Klondyke Formation in the Baguio District have La/Th values ranging from ~ 4 to 15.

Whole-rock rare earth element (REE) patterns are also used as indicators of source rock compositions. Taylor et al. (1986) did a study on post-Archean terrigenous sedimentary rocks taken from different source rock terranes with varying degrees of chemical weathering, sorting, and diagenesis. It was pointed out that there is uniformity of REE patterns regardless of sedimentation and diagenetic factors because REEs are immobile and are not soluble in water. Therefore, no interelement exchange can take place. In Fig. 6, a multielement diagram shows the element concentrations of the Lasala clastic rocks normalized to chondrite (Boynton 1984). This allows direct comparison of the Lasala samples to the average upper continental crust (UCC) (Taylor and McLennan 1985). Element patterns of the Lasala samples are similar with the UCC that are characterized by enrichment in LREEs and depletion in HREEs. Comparable multielement patterns are noted for the clastic rock samples from the Buruanga Peninsula in northwest Panay as well as for samples from the Nanxiong Basin in South China. In contrast, the field for the Baguio clastic rock samples displays a more flat character and the distinct absence of a Eu anomaly (Fig. 6). Such a pattern as shown by the Baguio clastic rocks is characteristic of sediments deposited in island arc environments (e.g., McLennan 1982; McLennan and Taylor 1984).

A distinct depletion in Eu relative to other REEs is also observed in the patterns, and this is usually attributed to silicic source rocks. A negative Eu anomaly is correlated with the transition of the upper continental crust from a mafic Archean one to a relatively silicic post-Archean variety through intracrustal differentiation (e.g., Fedo et al. 1996). This change produced K-rich granites, granodiorites, and other silicic rocks depleted in Eu which were then incorporated in terrigenous sedimentary rocks. The pronounced negative Eu anomaly observed in the patterns is due to the input of Eu-depleted granitic detritus into the sediments that formed the Lasala clastic rocks (e.g., Taylor and McLennan 1985; Rollinson 1993).

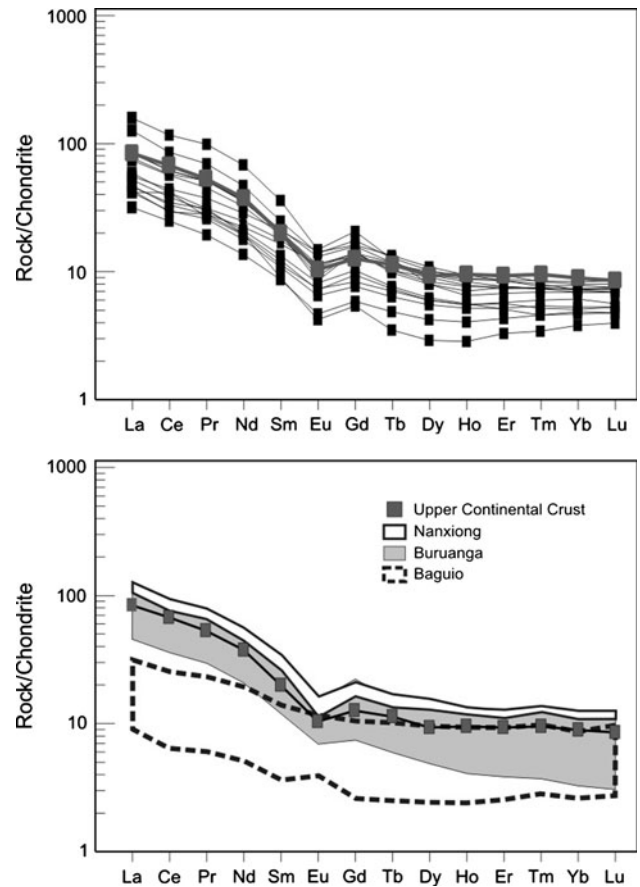


Fig. 6 **a** (Top) Chondrite-normalized multielement plot of the Lasala samples (black square) normalized to chondrite. Normalizing factors are from Evensen et al. (1978). The patterns showing enrichment in LREE, depletion in HREE, and negative Eu anomaly are consistent with derivation from a granodiorite upper continental crust composition. **b** (Bottom) Similar patterns are observed for the Nanxiong Basin and Buruanga clastic rocks. Samples derived from mafic igneous rocks show a more flat pattern and are marked by an absence of a distinct negative Eu anomaly. Nanxiong, Buruanga, and Baguio data are from Yan et al. (2007), Gabo et al. (2009) and Tam et al. (2005) respectively. See text for details

Provenance discrimination diagrams, REE patterns, and a negative Eu anomaly all point to a felsic provenance for the Lasala clastic sedimentary rocks.

Tectonic setting

Based on the Qt-F-L and Qm-F-Lt diagrams, the Lasala clastic rocks mostly plot within the craton interior and transitional continental field (Fig. 3c, d). These sedimentary rocks are derived from continental sediments deposited on either passive or active continental margin (e.g., Moss 1998; Tucker 2001). Some samples that occupy the recycled orogen field are attributed to derivation from the Halcon metamorphics which is believed to represent a metamorphosed piece of the Mainland Asia continental

crust. The interpretation of the latter is due to some samples that contain abundant polycrystalline quartz (Qp) compared with monocrystalline quartz (Qm) (e.g., Tucker 2001; Das et al. 2008). Consequently, these grains exhibit undulose extinction indicative of metamorphism. Petrographic analysis of Lasala clastic rocks, therefore, shows a continental source deposited on either passive or active continental margin. Modal plots of Palawan and Buruanga samples that are both continental in origin are shown together with the plots of the Lasala clastic rock samples to further affirm the continental signatures of the Lasala samples (Suzuki et al. 2000; Gabo et al. 2009) (Fig. 3c). In contrast, samples from the oceanic island arc-derived Klondyke Formation in the Baguio District clearly occupy the magmatic arc field (Fig. 3c).

Various studies involving geochemical discrimination parameters have proven useful in characterizing tectonic settings of terrigenous sedimentary rocks. On the basis of major oxides, Roser and Korsch (1986) utilized K_2O , Na_2O , and SiO_2 to establish the tectonic settings of sandstone and mudstone suites. Felsic rocks tend to have high concentrations of these compounds compared with mafic rocks. However, this tectonic diagram must be employed with caution because K_2O , Na_2O , and SiO_2 contents may be obscured by post-depositional processes such as silicification and K-metasomatism (Cullers et al. 1993; Fedo et al. 1995; Sugitani et al. 2006). Results from this diagram may only be deemed reliable if it complements the petrography of the samples (Roser and Korsch 1986). Significant hydrothermal veins that can be a source of secondary silica (e.g., Van den Boorn et al. 2007) were not encountered in the field during geologic mapping. Therefore, influence from silicification in the Lasala clastic rocks is unlikely. Petrographic analysis also confirms that the quartz crystals present in the samples are detrital rather than replacement silica due to silicification. Based on the A-CN-K ternary diagram (Fig. 4), six mudstone samples of the Lasala clastic rocks underwent slight K-metasomatism, and so these samples are excluded in the K_2O/Na_2O versus SiO_2 diagram. Plots of the Lasala clastic rocks on this diagram show passive and active continental margin tectonic settings (Fig. 7a). On the Th-Co-Zr/10 plot proposed by Bhatia and Crook (1986) for tectonic setting discrimination, most of the samples are found within the continental island arc (CIA) and passive margin (PCM) fields (Fig. 7b).

Although the Lasala clastic rock samples point to a chiefly continental tectonic setting, the plots straddle between active continental margin (ACM) and passive margin (PM). Middle Jurassic to mid-Cretaceous tectonic reconstructions of Holloway (1982) suggested an active continental margin setting for the southeastern portion of Mainland Asia where a northwest-dipping subduction zone

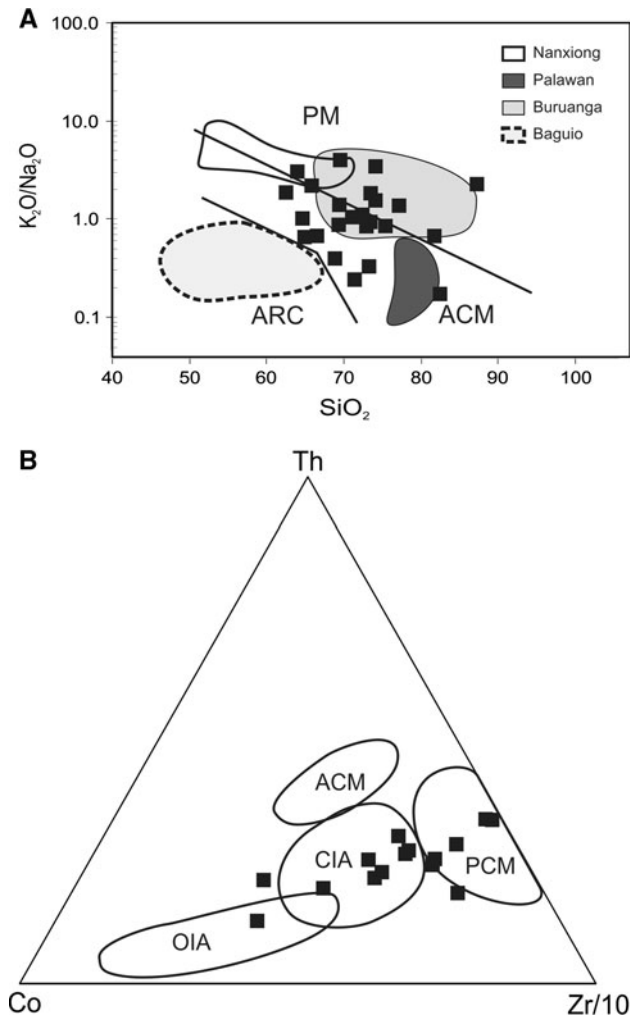


Fig. 7 a The Mindoro samples when plotted on the K_2O/Na_2O versus SiO_2 diagram mostly fall within the active continental margin (ACM) and passive margin (PM) tectonic settings. The fields for Naxiong, Palawan, and Buruanga also plot within the same ACM and PM fields. In contrast, samples from the Klondyke Formation in Baguio distinctly fall within the arc field. b On the Th-Co-Zr/10 diagram, the majority of the Lasala samples occupy the CIA and PCM fields. ACM active continental margin, OIA oceanic island arc, CIA continental island arc, PCM passive margin

commenced as a consequence of a spreading event involving Australia and a continental fragment down south. This subduction episode on this part of Mainland Asia produced a subparallel magmatic arc of calc-alkalic extrusive and intermediate to acid intrusives preserved in southeastern Vietnam and eastern China (Hamilton 1979; Holloway 1982). However, this active tectonic setting ceased during the Late Cretaceous in exchange of a new northward-dipping subduction zone in Sumatra-Java-southeast Borneo (Holloway 1982). Reconstructions during the Paleocene in the southeastern portion of Mainland Asia revealed a relatively passive margin (Holloway 1982; Hall 2002; Queaño et al. 2007). This implies that the Eocene

Lasala Formation was deposited in a chiefly passive continental margin, and samples that plot within the ACM field are believed to have received detritus from rocks generated at an older active margin. Petrographic expression of this inherited active margin signature is the basaltic lithic fragments (2–12%) that were incorporated in the samples.

Tectonic implications

Mindoro continental block

Although several papers have suggested that only southwestern Mindoro is continental (e.g., Hall 2002; Queaño et al. 2007) and northeastern Mindoro is of Philippine Sea Plate affinity (e.g., Rangin et al. 1990; Pubellier et al. 1996), the Lasala Formation provides the first tangible on-land proof that it is in fact the entire island that is continental. The Palawan continental block is widely accepted as a continental fragment that rifted off from the southern margin of Mainland Asia consequent to the opening of the South China Sea. This idea is supported by paleomagnetic data (e.g., Alamasco et al. 2000), seismic and seafloor magnetic anomaly data (e.g., Taylor and Hayes 1980; Holloway 1982), and stratigraphic correlation across the region (e.g., Holloway 1982; Zamoras and Matsuoka 2004). The oldest rock suite in the Palawan continental block is a Middle Permian sedimentary sequence of sandstones, tuff, and slates whose metamorphosed equivalent is believed to be the Halcon metamorphics of Mindoro (Hashimoto and Sato 1968; Holloway 1982). Holloway (1982) suggested that the slightly metamorphosed shales and siltstones and minor fossiliferous carbonates also of Permian age exposed in eastern China, Hongkong, and eastern Guangdong are related to this sedimentary suite. Late Triassic Indosinian orogeny brought about by the suturing of Indochina and South China blocks produced acidic igneous intrusions near the Red River suture zone and within Palawan and Mindoro (Holloway 1982; Knittel et al. 2010). A northwest-dipping subduction zone along the southeastern Mainland Asia margin transpired in the Middle Jurassic to Mid-Cretaceous and was manifested through a series of calc-alkalic extrusions and intermediate to acid intrusions exposed only in southeastern Vietnam and eastern China (Hamilton 1979; Holloway 1982; Yu et al. 2006). Subduction ceased in Late Cretaceous and marked the beginning of continental crust attenuation in the southern margin of Mainland Asia that continued until Eocene (Holloway 1982). This created sedimentary successions of passive continental setting in both Mainland Asia and Palawan and Mindoro (Holloway 1982; Suzuki et al. 2000; Yan et al. 2007). Neither tectonic occurrences nor sedimentary rock deposition events were observed

common to Mainland Asia and Palawan continental block in the late Paleogene because it is believed that Palawan continental block completed its last phase of rifting from Mainland Asia and began its southeastward motion up to its present position as a consequence of the opening of the South China Sea (Holloway 1982). Based on magnetic lineations, Taylor and Hayes (1983) proposed that seafloor spreading of the South China Sea started during the mid- to late Oligocene up to Middle Miocene. A more recent study suggests an older age of late Eocene for the rifting and opening of the oceanic basin due to the recognition of magnetic lineations in the northernmost South China Sea near the Formosa Canyon and the northern end of the Manila Trench (Hsu et al. 2004). Subduction of the South China Sea crust beneath the Manila Trench brought the Palawan continental block in collision with the Philippine Mobile Belt during the late Early Miocene to early Middle Miocene (Holloway 1982).

The Eocene Lasala Formation is the oldest sedimentary sequence in northwest Mindoro which Sarewitz and Karig (1986) mapped as part of the Philippine Mobile Belt. Because of its age, it is assumed that the Eocene Lasala Formation was deposited prior to the collision event. Petrographic study shows that the sandstones were mainly derived from silicic or felsic source rocks. Whole-rock major and trace element analyses also point to a felsic and quartzose recycled provenance. The continental character of the Lasala clastic rocks is further supported by tectonic discrimination diagrams that indicate a chiefly passive with inherited active continental margin paleo-setting. Because of the wide distribution of the Lasala Formation across the island, it is concluded that the whole island of Mindoro is continent derived and therefore forms part of the Palawan continental block.

Locating the collision boundary

Considering the entirety of Mindoro, as being continental and part of the Palawan block implies that the collision boundary between the Palawan continental block and the Philippine Mobile Belt should be located farther east of Mindoro. Several previous geophysical studies have looked into establishing the position of this collision margin in central Philippines. Available geophysical data were thus culled in order to look at anomalies that may help delineate the collision boundary. Based on seismicity, shear wave velocity and regional gravity data, thickened crust is noted from Bicol extending southwestward to Panay island through the Sibuyan—Masbate area (Wu et al. 2004; Dimalanta and Yumul 2008). When the crustal thickness data were first evaluated, it was reported that the collision did not seem to have resulted in crustal thickening because thickened crust was not observed in the Mindoro-Romblon

region, which is the site of collision (Dimalanta and Yumul 2004). Recent geological and geochemical data from the Romblon Island Group have suggested that the easternmost boundary of the collision lies further east of Sibuyan Island. It is at this site where thickened crust can be observed (e.g., Dimalanta and Yumul 2003, 2004; Wu et al. 2004). On the bathymetric map, a depression or trough of up to ~1,000 m is observed in the area between Sibuyan and Masbate islands. This bathymetric low is characterized by a low Bouguer anomaly value, i.e., 50 mGal, compared with the 100 mGal to the west and east of this depression (Sonido 1981). These variations in bathymetry and gravity values along with the observed variations in crustal thickness within the central Philippine region may offer additional constraints in delimiting the boundary of the collision zone.

Regional correlations and recommendations

In the context of Southeast Asia's tectonic development, Mindoro island, together with the islands of Taiwan, Palawan, and western Panay, formed a contiguous group of landmasses along the southeastern margin of the Asian Continent. Most palinspastic reconstruction studies suggest that during the early part of the Mesozoic, this margin was the site of active subduction (e.g., Holloway 1982). Reconstructions for the Paleogene period show that as late as the Eocene, this continental periphery was relatively passive, with most tectonism occurring farther south along the Philippine Sea Plate—Australian block boundary (e.g., Hall 2002; Queaño et al. 2007). Hence, considering these tectonic models, the Lasala Formation would have been deposited in a basin flanking southeast China, Taiwan, and Palawan. This implies that sedimentary rocks of correlatable age, character, and history to the Lasala Formation may be present in those areas as well.

Eocene sedimentary rocks in northern Taiwan (Hsitsun and Szeleng Formations) are suggested to have been derived from Jurassic-Cretaceous and Paleozoic granitic plutons of southeast China (Shao et al. 2009). The older Hsitsun Formation is composed of well-foliated dark gray slate and phyllitic slate with interbeds of dark colored, fine-grained, hard quartzose sandstone that are more abundant in the lower part of the formation (Central Geological Survey of Taiwan 2010). The younger Szeleng Formation is generally arkosic to subarkosic and is characterized by thick-bedded, light gray quartzitic sandstone, or quartzite intercalated with dark gray argillite or slate (Central Geological Survey of Taiwan 2010).

Correlation of these rocks, and others of similar age and characteristics in the region, can provide a more complete understanding of east and southeast Asian margin tectonics. The position of this formation within the regional

stratigraphy has the potential to provide crucial information on the poorly documented Cretaceous-Tertiary boundary of the Philippines and southeast Asia as a whole. Therefore, province-link investigations that include southeast China, Taiwan, Palawan, and Malaysia can likely address this research gap.

Conclusions

Petrographic and geochemical analyses have distinguished the Lasala Formation of northwest Mindoro as being derived from a continental source developed in a continental margin tectonic setting. The mineralogical assemblage, dominantly characterized by the abundance of quartz minerals, suggests felsic sources which effectively indicate a continental origin. Ternary petrographic and tectonic function discrimination diagrams similarly point to continental tectonic settings. Geochemical characteristics such as high SiO₂ content, low Al₂O₃/TiO₂ and La/Th, low Co, Cr, and Ni elemental abundances, negative Eu anomalies and depletion in LREEs indicate a felsic or silicic provenance. The best fit line through the data points on the A-CN-K diagram is also consistent with a granodioritic upper continental crust composition. Tectonic discrimination diagrams similarly indicate that the sediments of Lasala Formation were derived from continental sources, but they straddle both active and passive margin characteristics. Correlation of this mixed signature with previous paleogeographic studies of southeast Asia shows that the Lasala sedimentary rocks were deposited in a passive margin setting where products of older active margin tectonic processes were also being shed. Results from this study provide the first tangible on-land proof that the whole island of Mindoro is continent derived and forms part of the Palawan Block.

Acknowledgments We acknowledge the financial support given by the Department of Science and Technology–Philippine Council for Industry and Energy Research and Development (DOST–PCIERD) and the University of the Philippines–National Institute of Geological Sciences (UP–NIGS). Logistic and field support was extended by the provincial government of Mamburao, Occidental Mindoro. Special thanks to Prof. Mei–Fu Zhou of The University of Hongkong, Prof. Tsanyao Frank Yang of National Taiwan University, Dr. Allan Gil Fernando of UP–NIGS, and Mr. Raymond Ancog of MGB for the analysis of the samples. Productive discussions from members of the Rushurgent Working Group of the National Institute of Geological Sciences are acknowledged with thanks.

References

- Agadier-Zepeda MA, Tumanda FP, Revilla A (1992) The Paleogene-Neogene sequence of southwest Mindoro island, Philippines—stratigraphy and events. Bureau of Mines, unpublished report

- Alamasco JN, Fuller RM, Frost G (2000) Paleomagnetism of Palawan, Philippines. *J Asian Earth Sci* 18:369–389
- Armstrong-Altrin JS, Verma SP (2005) Critical evaluation of six tectonic setting discrimination diagrams using geochemical data of Neogene sediments from known tectonic settings. *Sed Geol* 177:115–129
- Asiedu DK, Suzuki S, Shibata T (2000) Provenance of sandstones from the lower Cretaceous Sasayama group, Inner Zone of Southwest Japan. *Sed Geol* 131:9–24
- Bhatia MR (1983) Plate tectonics and geochemical composition of sandstones. *J Geol* 91:611–627
- Bhatia MR, Crook KAW (1986) Trace element characteristics of graywackes and tectonic setting discrimination of sedimentary basins. *Contrib Mineral Petrol* 92:181–193
- Bird PB, Quinton NA, Beeson MN, Bristow C (1993) Mindoro: a rifted microcontinent in collision with the Philippines volcanic arc; basin evolution and hydrocarbon potential. *J SE Asian Sci* 8:449–468
- Boynton WV (1984) Cosmochemistry of the rare earth elements: meteorite studies. In: Henderson P (ed) *Rare Earth Element Geochemistry*, Elsevier Science Publishing, Amsterdam, pp 63–114
- Central Geological Survey of Taiwan (2010) Stratigraphy of the northern part of the Hsuehshan Range Belt. http://www.moeacgs.gov.tw/english2/twgeol/twgeol_western_13.jsp. Accessed 20 Aug 2010
- Chakrabarti G, Debashish S, Blanca B, Subhajt S (2009) Provenance and weathering history of Mesoproterozoic clastic sedimentary rocks from the Basal Gulcheru Formation, Cuddapah Basin. *J Geol Soc In* 74:119–130
- Crook KAW (1974) Lithogenesis and geotectonics: the significance of compositional variations in flysch arenites (graywackes). In: Dott RH, Shaver RH (eds) *Modern and ancient geosynclinal sedimentation*. *Soc Sed Geol (SEPM) Spec Publ* 19, pp 304–310
- Cullers RL, DiMarco MJ, Lowe DR, Stone J (1993) Geochemistry of a silicified, felsic volcanoclastic suite from the early Archaean Panorama Formation, Pilbara Block, Western Australia: an evaluation of depositional and post-depositional processes with special emphasis on the rare-earth elements. *Precamb Res* 60:99–116
- Das SK, Routh J, Roychoudhury AN, Klump JV (2008) Major and trace element geochemistry in Zeekoevlei, South Africa: a lacustrine record of present and past processes. *Appl Geochem* 23:2496–2511
- Deru X, Xuexiang G, Pengchun L, Guanghao C, Bin X, Bachlinski R, Zhuanli H, Gonggu F (2007) Mesoproterozoic-Neoproterozoic transition: geochemistry, provenance and tectonic setting of clastic sedimentary rocks on the SE margin of the Yangtze Block, South China. *J Asian Earth Sci* 29:637–650
- Dickinson WR (1985) Interpreting provenance relations from detrital modes of sandstones. In: Zuffa GG (ed) *Provenance of Arenites*. Reidel Publishing Company, Dordrecht, pp 333–361
- Dickinson WR, Suczek CA (1979) Plate tectonics and sandstone compositions. *Am Assoc Petrol Geol Bull* 63:2164–2182
- Dimalanta CB, Yumul GP Jr (2003) Magmatic and amagmatic contributions to crustal growth of an island arc system: the Philippine example. *Int Geol Rev* 45:922–935
- Dimalanta CB, Yumul GP Jr (2004) Crustal thickening in an active margin setting (Philippines): the whys and the hows. *Episodes* 27:260–264
- Dimalanta CB, Yumul GP Jr (2008) Crustal thickness and adakite occurrence in the Philippines: is there a relationship? *Isl Arc* 17:421–431
- Evensen NM, Hamilton PJ, O'niions RK (1978) Rare-earth abundances in chondritic meteorites. *Geochim Cosmochim Acta* 42:1199–1212. doi:10.1016/0016-7037(78)90114-X
- Faundez V, Herve F, Lacassie JP (2002) Provenance and depositional setting of pre-Late Jurassic turbidite complexes in Patagonia, Chile. *N Z J Geol Geophys* 45:411–425
- Faure M, Marchiader Y, Rangin C (1989) Pre-Eocene synmetamorphic structure in the Mindoro-Romblon-Palawan area, West Philippines, and implications for the history of Southeast Asia. *Tectonics* 8:963–969
- Fedo CM, Nesbitt HW, Young GM (1995) Unraveling the effects of potassium metasomatism in sedimentary rocks and paleosols, with implications for paleoweathering conditions and provenance. *Geology* 23:921–924
- Fedo CM, Eriksson KA, Krogstad EJ (1996) Geochemistry of shales from the Archean (3.0 Ga) Buhwa Greenstone belt, Zimbabwe: implication for provenance and source area weathering. *Geochim Cosmochim Acta* 60:1751–1763
- Folk RL (1965) *Petrology of sedimentary rocks*. Hemphill Publishing Company, Austin, Texas
- Gabo JAS, Dimalanta CB, Asio MGS, Queaño KL, Yumul GP Jr, Imai A (2009) Geology and geochemistry of the clastic sequences from Northwestern Panay (Philippines): implications for provenance and geotectonic setting. *Tectonophysics* 479:111–119
- Gu XX, Liu JM, Zheng MH, Tang JX, Qi L (2002) Provenance and tectonic setting of the Proterozoic turbidites in Hunan, South China: geochemical evidence. *J Sed Res* 72:393–407
- Hall R (2002) Cenozoic geological and plate tectonic evolution of SE Asia and the SW Pacific: computer-based reconstructions, model and animations. *J Asian Earth Sci* 20:353–421
- Hamilton W (1979) *Tectonics of the Indonesian Region*. Geological survey professional paper 1078
- Hashimoto W (1981) Geologic development of the Philippines. In: Kobayashi T, Toriyama R, Hashimoto W (eds) *Geol Paleontol SE Asia* 22, pp 83–170
- Hashimoto W, Sato T (1968) Contribution to the geology of Mindoro and Neighboring Islands, the Philippines. *Geol Paleontol SE Asia LXVI* 5:192–210
- Holloway NH (1982) North Palawan block, Philippines: its relation to Asian mainland and role in evolution of South China Sea. *Am Assoc Petrol Geol Bull* 16:1355–1383
- Hossain HMZ, Roser BP, Kimura JI (2010) Petrography and whole-rock geochemistry of the Tertiary Sylhet succession, northeastern Bengal Basin, Bangladesh: provenance and source area weathering. *Sed Geol* 228:171–183
- Hsu SK, Yeh YC, Doo WB, Tsai CH (2004) New bathymetry and magnetic lineations identifications in the northernmost South China Sea and their tectonic implications. *Mar Geophys Res* 25:24–44. doi:10.1007/s11001-005-0731-7
- Hunstan-Mapila P, Kampunzu AB, Vink B, Ringrose S (2005) Cryptic indicators of provenance from the geochemistry of the Okavango Delta sediments, Botswana. *Sed Geol* 174:128–148
- Jumawan FT, Yumul GP Jr, Tamayo RA Jr (1998) Using geochemistry as a tool in determining the tectonic setting and mineralization potential of an exposed upper-mantle crust sequence: example from the Amnay Ophiolitic Complex in Occidental Mindoro, Philippines. *J Geol Soc Phil* 53:24–48
- Kasanzu C, Maboko MAH, Many S (2008) Geochemistry of fine-grained clastic sedimentary rocks of the Neoproterozoic Ikorongo Group, NE Tanzania: implications for provenance and source rock weathering. *Precamb Res* 164:201–213
- Kawano Y, Akiyama M, Ikawa T, Roser BP, Imaoka T, Ishioka J, Yuhara M, Hamamoto T, Havasaka Y, Kagami H (2006) Whole rock geochemistry and Sr isotopic compositions of Phanerozoic sedimentary rocks in the inner zone of the Southwest Japan Arc. *Gondwana Res* 9:126–141
- Knittel U, Hung CH, Yang TF, Iizuka Y (2010) Permian arc magmatism in Mindoro, the Philippines: an early Indosinian

- event in the Palawan Continental Terrane. *Tectonophysics* 493:113–117. doi:[10.1016/j.tecto.2010.07.007](https://doi.org/10.1016/j.tecto.2010.07.007)
- Lee JI (2009) Geochemistry of shales of the upper Cretaceous Hayang group, SE Korea: implications for provenance and source weathering at an active continental margin. *Sed Geol* 215:1–12
- Lee JI, Lee YI (2003) Geochemistry and provenance of lower Cretaceous Sindong and Hayang mudrocks, Gyeongsang Basin, Southeastern Korea. *Geosci J* 7:107–122
- Liang M, Guo Z, Kahmann AJ, Oldfield F (2009) Geochemical characteristics of the Miocene eolian deposits in China: their provenance and climate implications. *Geochem Geophys Geosyst* 10. doi:[10.1029/2008GC002331](https://doi.org/10.1029/2008GC002331)
- Liu S, Lin G, Liu Y, Zhou Y, Gong F, Yan Y (2007) Geochemistry of middle oligocene–pliocene sandstones from the Nanpu Sag, Bohai Bay Basin (Eastern China): implications for provenance, weathering, and tectonic setting. *Geochem J* 41:359–378
- McLennan SM (1982) On the geochemical evolution of sedimentary rocks. *Chem Geol* 37:335–350
- McLennan SM, Taylor SR (1984) Archaean sedimentary rocks and their relation to the composition of the Archaean continental crust. In: Kroner A, Hanson GN, Goodwin AM (eds) *Archaean Geochem*. Springer, New York, pp 47–71
- McLennan SM, Nance WB, Taylor SR (1980) Rare earth element–thorium correlations in sedimentary rocks, and the composition of the continental crust. *Geochim Cosmochim Acta* 44:1833–1839
- Meinhold G, Kostopoulos D, Reischmann T (2007) Geochemical constraints on the provenance and depositional setting of sedimentary rocks from the islands of Chios, Inousses and Psara, Aegean Sea, Greece: implications for the evolution of Palaeotethys. *J Geol Soc* 164:1145–1163
- Metal Mining Agency of Japan—Japan International Cooperation Agency (MMAJ-JICA) (1984) Report on the geological survey of Mindoro Island consolidated report 57
- Mongelli G, Salvatore C, Perri F, Sonnino M, Perrone V (2006) Sedimentary recycling, provenance and paleoweathering from chemistry and mineralogy of Mesozoic continental redbed mudrocks, Peloritani mountains, southern Italy. *Geochem J* 40:197–209
- Moss S (1998) Embaluh Group turbidites in Kalimantan: evolution of a remnant oceanic basin in Borneo during the Late Cretaceous to Palaeogene. *J Geol Soc Lond* 155:509–524
- Nagarajan R, Madhavaraju J, Raghavendra N, Armstrong-Aldrin JS, Moutte J (2007) Geochemistry of Neoproterozoic shales of the Rabanpalli formation, Bhima Basin, Northern Karnataka, southern India: implications for provenance and paleoredox conditions. *Revista Mexicana de Ciencias Geológicas* 24:150–160
- Nesbitt HW, Young GM (1982) Early Proterozoic climates and plate motions inferred from major element chemistry of lutites. *Nature* 299:715–717
- Nesbitt HW, Young GM (1996) Petrogenesis of sediments in the absence of chemical weathering: effects of abrasion and sorting on bulk composition and mineralogy. *Sedimentology* 43:341–358
- Nesbitt HW, Young GM, McLennan SM, Keays RR (1996) Effects of chemical weathering and sorting on the petrogenesis of siliciclastic sediments, with implication for provenance studies. *J Geol* 104:525–542
- Pubellier M, Quebral Q, Aurelio M, Rangin C (1996) Docking and post-docking escape tectonics in the southern Philippines. In: Hall R, Blundell D (eds) *Tectonic evolution of Southeast Asia*. *Geol Soc Lond Spec Publ* 106, pp 511–523
- Queaño KL, Ali JR, Milsom J, Aitchison JC, Pubellier M (2007) North Luzon and the Philippine sea plate motion model: insights following magnetic, structural and age-dating investigations. *J Geophys Res* 112:B05101. doi:[10.1029/2006Jb004506](https://doi.org/10.1029/2006Jb004506)
- Rahman MJJ, Suzuki S (2007) Geochemistry of sandstones from the Miocene Surma group, Bengal Basin, Bangladesh: implications for provenance, tectonic setting and weathering. *Geochem J* 41:415–428
- Rangin C, Stephan JF, Muller C (1985) Middle Oligocene oceanic crust of South China Sea jammed into Mindoro collision zone (Philippines). *Geology* 13:425–428
- Rangin C, Jolivet L, Pubellier M, TethysPacificWorking Group (1990) A simple model for the tectonic evolution of Southeast Asia and Indonesia region for the last 43 m.y. *Bull Geol Soc France* 8:889–905
- Reatigui K, Martinez M, Esteves I, Gutierrez JV, Martinez A, Melendez W, Urbani F (2005) Geochemistry of the Mirador Formation (Late Eocene–Early Oligocene), southwestern Venezuela: Chemostratigraphic constraints on provenance and the influence of the sea level. *Geochem J* 39:213–226
- Rollinson HR (1993) *Using geochemical data: evaluation, presentation, interpretation*. Longman Scientific and Technical Publishing, New York
- Roser BP, Korsch RJ (1986) Determination of tectonic setting of sandstone–mudstone suites using SiO₂ content and K₂O/Na₂O ratio. *J Geol* 94:635–650
- Roser BP, Korsch RJ (1988) Provenance signatures of sandstone–mudstone suites determined using discriminant function analysis of major-element data. *Chem Geol* 67:119–139
- Sarewitz DR, Karig DE (1986) Processes of allochthonous terrane evolution, Mindoro Island, Philippines. *Tectonics* 5:525–552
- Shao W, Chen W, Chung S (2009) Detrital zircon U–Pb isotopic constraints on the source provenance of the Eocene–Miocene sedimentary rocks, northern Taiwan. *American Geophysical Union, Fall Meeting 2009*, abstract #V33B-2041
- Soejima T (1999) Application of rock powder pellet analysis using high-sensitivity XRF analysis machine and chemical weathering. M.Sc. Thesis, Department of Earth Resources Engineering, Kyushu University, Fukuoka, Japan, 35 pp. (in Japanese)
- Sonido EP (1981) The state of gravity works in the Philippines. *J Geol Soc Phil* 35:37–50
- Sugitani K, Yamashita F, Nagaoka T, Minami M, Yamamoto K (2006) Geochemistry of heavily altered Archean volcanic and volcanoclastic rocks of Warrawoona Group, at Mt. Goldsworthy in the Pilbara Craton, Western Australia: Implications for alteration and origin. *Geochem J* 40:523–535
- Suzuki S, Takemura S, Yumul GP Jr, David SD Jr, Asiedu DK (2000) Composition and provenance of the upper cretaceous to Eocene sandstones in Central Palawan, Philippines: constraints on the Tectonic development of Palawan. *Isl Arc* 9:611–626
- Tam TA, Yumul GP Jr, Ramos EGL, Dimalanta CB, Zhou MF, Suzuki S (2005) Rare earth element geochemistry of the Zigzag–Klondyke sedimentary formations: clues to the evolution of the Baguio Mineral District (Luzon), Philippines. *Resour Geol* 55:217–224
- Taylor B, Hayes DE (1980) The tectonic evolution of the South China Basin. In: Hayes DE (ed) *The tectonic and geologic evolution of Southeast Asian seas and islands*. *Am Geophys Union Monogr* 23, pp 89–104
- Taylor B, Hayes DE (1983) Origin and history of the South China Sea Basin. In: Taylor B, Hayes DE (eds) *The tectonic and geologic evolution of Southeast Asian seas and islands*. *Am Geophys Union Monogr* 2, pp 23–56
- Taylor SR, McLennan SM (1985) *The continental crust: its composition and evolution*. Blackwell, Oxford
- Taylor SR, Rudnick RL, McLennan SM, Eriksson K (1986) Rare earth element patterns in Archean high-grade metasediments and their tectonic significance. *Geochim Cosmochim Acta* 50:2267–2279

- Teves JS (1954) The pre-tertiary geology of southern oriental Mindoro. *Phil Geologist* 8:2–36
- Tucker ME (2001) *Sedimentary Petrology*, 3rd edn. Blackwell Publishing, Oxford, pp 48–54
- Van den Boorn SHJM, Van Bergen MJ, Nijman W, Vroon PZ (2007) Dual role of seawater and hydrothermal fluids in early Archean chert formation: evidence from silicon isotopes. *Geology* 35:939–942
- Van Hattum MWA, Hall R, Pickard AL, Nichols GJ (2006) Southeast Asian sediments not from Asia: provenance and geochronology of north Borneo sandstones. *Geology* 34:589–592
- Wu HH, Tsai YB, Lee TY, Lo CH, Hsieh CH (2004) 3-D shear wave velocity structure of the crust and upper mantle in South China Sea and its surrounding regions by surface wave dispersion analysis. *Mar Geophys Res* 25:5–27
- Yan Y, Xia B, Lin G, Cui X, Hu X, Yan P, Zhang F (2007) Geochemistry of the sedimentary rocks from the Nanxiong Basin, South China and implications for the provenance, paleoenvironment and paleoclimate at the K/T boundary. *Sed Geol* 197:127–140
- Yu X, Ganguo W, Da Z, Tiezeng Y, Yongjun D, Longwu W (2006) Cretaceous extension of the Ganhang Tectonic Belt, southeastern China: constraints from geochemistry of volcanic rocks. *Cretaceous Res* 27:663–672
- Yumul GP Jr, Dimalanta CB, Marquez EJ, Queaño KL (2008) Onland signatures of the Palawan microcontinental block and Philippine mobile belt collision and crustal growth process: a review. *J Asian Earth Sci* 34:610–623
- Yumul GP Jr, Jumawan FT, Dimalanta CB (2009) Geology, geochemistry and chromite mineralization potential of the Amnay Ophiolitic Complex, Mindoro, Philippines. *Resour Geol* 59:263–281
- Zamoras LR, Matsuoka A (2004) Accretion and postaccretion tectonics of the Calamian Islands, North Palawan block, Philippines. *Isl Arc* 13:506–519